

Structural, mechanical, electronic properties, and Debye temperature of quaternary carbide Ti_3NiAl_2C ceramics under high pressure: A first-principles study

Diyou Jiang(姜迪友), Wenbo Xiao(肖文波), and Sanqiu Liu(刘三秋)

Citation: Chin. Phys. B, 2021, 30 (**3**): 036202. DOI: 10.1088/1674-1056/abca20
Journal homepage: http://cpb.iphy.ac.cn; http://iopscience.iop.org/cpb

What follows is a list of articles you may be interested in

Structural, mechanical, and electronic properties of Zr-Te compounds from first-principles calculations

Peng Wang(王鹏), Ning-Chao Zhang(张宁超), Cheng-Lu Jiang(蒋城露), Fu-Sheng Liu(刘福生), Zheng-Tang Liu(刘正堂), Qi-Jun Liu(刘其军)
Chin. Phys. B, 2020, 29 (**7**): 076201. DOI: 10.1088/1674-1056/ab8da7

Balancing strength and plasticity of dual-phase amorphous/crystalline nanostructured Mg alloys

Jia-Yi Wang(王佳怡), Hai-Yang Song(宋海洋), Min-Rong An(安敏荣), Qiong Deng(邓琼), Yu-Long Li(李玉龙)
Chin. Phys. B, 2020, 29 (**6**): 066201. DOI: 10.1088/1674-1056/ab84d5

Effects of helium implantation on mechanical properties of $(Al_{0.31}Cr_{0.20}Fe_{0.14}Ni_{0.35})O$ high entropy oxide films

Zhao-Ming Yang(杨朝明), Kun Zhang(张坤), Nan Qiu(裘南), Hai-Bin Zhang(张海斌), Yuan Wang(汪渊), Jian Chen(陈坚)
Chin. Phys. B, 2019, 28 (**4**): 046201. DOI: 10.1088/1674-1056/28/4/046201

First-principles investigations on structural stability, mechanical, and thermodynamic properties of LaT_2Al_{20} (T=Ti, V, Cr, Nb, and Ta) intermetallic cage compounds

Shanyu Quan(权善玉), Xudong Zhang(张旭东), Cong Liu(刘聪), Wei Jiang(姜伟)
Chin. Phys. B, 2018, 27 (**12**): 126201. DOI: 10.1088/1674-1056/27/12/126201

Investigation of mechanical properties of twin gold crystal nanowires under uniaxial load by molecular dynamics method

Guo-Wei Zhang(张国伟), Zai-Lin Yang(杨在林), Gang Luo(罗刚)
Chin. Phys. B, 2016, 25 (**8**): 086203. DOI: 10.1088/1674-1056/25/8/086203

Structural, mechanical, electronic properties, and Debye temperature of quaternary carbide Ti_3NiAl_2C ceramics under high pressure: A first-principles study*

Diyou Jiang(姜迪友)[1,2,†], Wenbo Xiao(肖文波)[1,2], and Sanqiu Liu(刘三秋)[3]

[1] *Key Laboratory of Nondestructive Testing, Ministry of Education, Nanchang Hangkong University, Nanchang* 330063, *China*
[2] *Fujian Science & Technology Innovation Laboratory for Energy Devices of China (21C-LAB), Ningde* 352100, *China*
[3] *Department of Physics, Nanchang University, Nanchang* 330047, *China*

(Received 2 October 2020; revised manuscript received 2 November 2020; accepted manuscript online 13 November 2020)

Quaternary carbide Ti_3NiAl_2C ceramics has been investigated as a potential nuclear fusion structural material, and it has advantages in certain aspects compared with Ti_2AlC, Ti_3AlC_2, and Ti_3SiC_2 structural materials. In this paper, quaternary carbide Ti_3NiAl_2C ceramics is pressurized to investigate its structural, mechanical, electronic properties, and Debye temperature. Quaternary carbide Ti_3NiAl_2C ceramics still maintains a cubic structure under pressure (0–110 GPa). At zero pressure, quaternary carbide Ti_3NiAl_2C ceramics only has three bonds: Ti–Al, Ni–Al, and Ti–C. However, at pressures of 20 GPa, 30 GPa, 40 GPa, 60 GPa, and 70 GPa, new Ti–Ni, Ti–Ti, Al–Al, Ti–Al, and Ti–Ti bonds form. When the pressure reaches 20 GPa, the covalent bonds change to metallic bonds. The volume of quaternary carbide Ti_3NiAl_2C ceramics can be compressed to 72% of its original volume at most. Pressurization can improve the mechanical strength and ductility of quaternary carbide Ti_3NiAl_2C ceramics. At 50–60 GPa, its mechanical strength can be comparable to pure tungsten, and the material changes from brittleness to ductility. However, the degree of anisotropy of quaternary carbide Ti_3NiAl_2C ceramics increases with the increasing pressure. In addition, we also investigated the Debye temperature, density, melting point, hardness, and wear resistance of quaternary carbide Ti_3NiAl_2C ceramics under pressure.

Keywords: quaternary carbide Ti_3NiAl_2C ceramics, structural properties, mechanical properties, electronic properties, Debye temperature, first-principles

PACS: 62.20.−x, 62.20.de, 62.20.fk, 62.20.mj **DOI:** 10.1088/1674-1056/abca20

1. Introduction

$M_{n+1}AX_n$ phases (M represents the early transition metal of B group, n represents 1/2/3, A stands for an element of A group, and X is C or N) have both metallic and ceramic properties with its hexagonal close-packed structure, which have attracted great interest from researchers due to its excellent performances such as high melting point, high temperature stability, high temperature resistant to oxidation, high corrosion resistance, high elastic modulus, significant machinability, excellent resistant to thermal shock, good thermal and electrical conductivity, low density and micro-ductility at room temperature.[1–10] In addition, $M_{n+1}AX_n$ phases also exhibit good radiation resistance,[11] especially at high temperatures,[12–15] and are considered as a potential structural material for nuclear fission and fusion reactors.[16–18] In the $M_{n+1}AX_n$ phases, many materials have been studied, such as Ti_2AlC, [19,20] Ti_3AlC_2 [21,22] and Ti_3SiC_2 [23,24] compounds.

On the other hand, the composite carbides of Ti_2A1C and Ti_3A1C formulations have high efficiency when used as abrasives for glass polishing. With nickel proposed as a possible binder, the research on the Ti–Ni–Al–C quaternary system began to arouse the interest of researchers. The quaternary system: titanium-nickel-aluminum-carbon (Ti_3NiAl_2C) was established for 1100 °C (quench), and a quaternary η-carbide with a lattice parameter of $a = 11.40$–11.463 Å was found to exist.[25] The H-phase Ti_2AlC and the perovskite phase Ti_3AlC are no longer stable in the presence of minor amounts of nickel.[25] Cubic Ti_3NiAl_2C compounds as quaternary carbide ceramics[25] may also have the characteristics of the $M_{n+1}AX_n$ phases. So far, however, this material has not been further investigated, especially in theory.

In addition, high pressure can cause a material to undergo phase changes that change its chemical and physical properties, such as structural, mechanical, thermodynamic, optical, electronic, and magnetic properties.[26–35] At the same time, computational materials science can be used to investigate the structure performance relationship and design materials since the traditional experimental design is expensive and time-consuming. Computer simulation can improve the chemical and physical properties of specific compounds and greatly reduce the number of components to be prepared and characterized.[36–43]

*Project supported by Fujian Science & Technology Innovation Laboratory for Energy Devices of China (21C-LAB) (Grant No. 21C-OP-202013), the National Natural Science Foundation of China (Grant No. 12064027), the International Science and Technology Cooperation Program of China (Grant No. 2015DFA61800), and the Scientific Research Fund of Jiangxi Provincial Education Department, China (Grant No. GJJ180973).

†Corresponding author. E-mail: jiangdiyou2005@163.com

© 2021 Chinese Physical Society and IOP Publishing Ltd

In this paper, our purpose is to improve the chemical and physical properties of cubic Ti_3NiAl_2C compounds through pressurization based on density functional theory. Therefore, we focus on investigating the effect of pressure on the mechanical properties of quaternary carbide Ti_3NiAl_2C ceramics.

2. Model and computational details

Figure 1 shows the crystal structure of cubic Ti_3NiAl_2C compounds, which belongs to the Fd-3m space group. The model of cubic Ti_3NiAl_2C compounds consists of 112 atoms, which including 16 C, 32 Al, 16 Ni, and 48 Ti atoms. The valence electron of C, Al, Ni, and Ti atoms is C-$2s^2 2p^2$, Al-$3s^2 3p^1$, Ni-$4s^2 3d^8$, and Ti-$4s^2 3d^2$, respectively. Using VASP software, the first principles method according to density functional theory (DFT) along with the plane-wave pseudopotential is used to complete the current calculations.[44,45] According to the projector augmented wave method (PAW),[46] it can characterize the relationship between core ions and valence electrons. The generalized gradient approximation (GGA) of Perdew and Wang (PW91) is used to calculate the exchange-correlation potentials.[47] $3\times3\times3$ Monkhorst–Pack meshes as sampling k-point in Brillouin-zone.[48] All calculated plane wave cutoff energy is set to 430 eV, and further increasing the cutoff energy has little effect on the energy. Gaussian smearing method is used for all calculations, and its smearing width is 0.05 eV.

According to the relationship between pressure and volume, the Birch–Murnaghan equation of state (EOS) can be expressed as[28,35,49]

$$P(V) = \frac{3B_0}{2}\left[\left(\frac{V_0}{V}\right)^{\frac{7}{3}} - \left(\frac{V_0}{V}\right)^{\frac{5}{3}}\right] \times\left\{1+\frac{3}{4}(B_0'-4)\left[\left(\frac{V_0}{V}\right)^{\frac{2}{3}}-1\right]\right\}, \quad (1)$$

where P is the pressure, V_0 is the volume at 0 GPa, V is the volume at different pressures, B_0 is the bulk modulus at 0 GPa, B_0' is the derivative of bulk modulus to pressure at 0 GPa. The B_0 and B_0' are obtained by the following relations:

$$B_0 = -V\left(\frac{\partial P}{\partial V}\right)_{P=0}, \quad B_0' = \left(\frac{\partial B}{\partial P}\right)_{P=0}. \quad (2)$$

According to Voigt–Reuss–Hill averaging scheme,[50–53] a series of required mechanical parameters can be obtained by fitting the elastic constants, such as bulk modulus (B), Young's modulus (E), shear modulus (G), Poisson's ratio (ν), anisotropy coefficients (A), and Cauchy pressure (C'). The equation constructed can be expressed as

$$B = (C_{11}+2C_{12})/3, \quad (3)$$

$$G_V = \frac{C_{11}-C_{12}+3C_{44}}{5}, \quad (4)$$

$$G_R = \frac{5(C_{11}-C_{12})C_{44}}{4C_{44}+3(C_{11}-C_{12})}, \quad (5)$$

$$G = \frac{G_V+G_R}{2}, \quad (6)$$

$$E = \frac{9BG}{3B+G}, \quad (7)$$

$$C' = \frac{C_{12}-C_{44}}{2}, \quad (8)$$

$$\nu = \frac{3B-2G}{2(3B+G)}, \quad (9)$$

$$A = \frac{2C_{44}}{C_{11}-C_{12}}. \quad (10)$$

Debye temperature (Θ_D) is an important parameter for studying the thermodynamic properties. Therefore, it is necessary to explore the Debye temperature of quaternary carbide Ti_3NiAl_2C ceramics at different pressures. Debye temperature can be expressed as[54]

$$\Theta_D = \frac{h}{k_B}\left[\frac{3n}{4\pi}\left(\frac{N_A\rho}{m}\right)\right]^{\frac{1}{3}} v_m, \quad (11)$$

where k_B is the Boltzmann constant, h is the Planck constant, N_A is the Avogadro number, ρ is the mass density, m is the molecular weight, n is total number of atoms per formula, and v_m is the average sound velocity.

The average sound velocity (v_m) can be acquired by the following equation:[54]

$$v_m = \left[\frac{1}{3}\left(\frac{2}{v_s^3}+\frac{1}{v_l^3}\right)\right]^{-\frac{1}{3}}, \quad (12)$$

where v_l is the longitudinal sound velocity and v_s is the shear sound velocity, which can be calculated based on the B and G. The equation constructed is as follows:[55]

$$v_s = (G/\rho)^{\frac{1}{2}}, \quad (13)$$

$$v_l = \left(\frac{3B+4G}{3\rho}\right)^{\frac{1}{2}}. \quad (14)$$

3. Results and discussion

3.1. Structural properties

As shown in Fig. 1, we pressurized and optimized the crystal structure of quaternary carbide Ti_3NiAl_2C ceramics with a pressure range of 0–110 GPa and an interval of 10 GPa. At the same time, the optimized atomic positions and crystal configurations are used as the model for the study of mechanical properties.

Table 1 lists the cell volumes and lattice constants of quaternary carbide Ti_3NiAl_2C ceramics at different pressures. The lattice constant 11.454 Å calculated for cubic Ti_3NiAl_2C ceramics at zero pressure is consistent with the experimental values 11.40–11.463 Å,[25] which indicates that our calculations are reliable. The Ti_3NiAl_2C ceramics still maintains a

cubic lattice at different pressures. The lattice constants of quaternary carbide Ti_3NiAl_2C ceramics decrease with the increase of pressure due to the shortened bond lengths, as shown in Fig. 2.

Table 1. The lattice constants a, b and c (Å), volume V (Å^3) of cubic Ti_3NiAl_2C compounds at different pressures, and the bulk modulus B_0 (GPa) and its pressure derivative B_0' at 0 GPa.

Pressure (GPa)	a	b	c	V	B_0	B_0' (GPa)
0	11.454	11.454	11.454	1502.69	164.58	3.47552
10	11.244	11.244	11.244	1421.54		
20	11.080	11.080	11.080	1360.35		
30	10.939	10.939	10.939	1309.13		
40	10.819	10.819	10.819	1266.39		
50	10.713	10.713	10.713	1229.41		
60	10.617	10.617	10.617	1196.81		
70	10.531	10.531	10.531	1167.80		
80	10.451	10.451	10.451	1141.42		
90	10.380	10.380	10.380	1118.27		
100	10.313	10.313	10.313	1096.77		
110	10.247	10.247	10.247	1075.79		

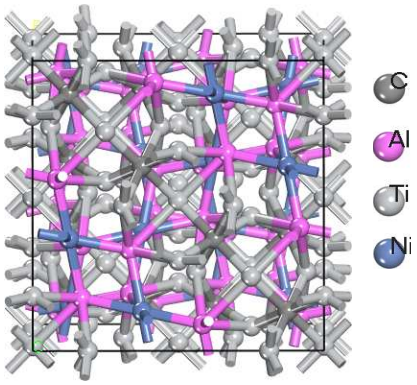


Fig. 1. Crystal structure model of cubic Ti_3NiAl_2C compounds. Black, pink, grey, and blue balls are C, Al, Ti, and Ni atoms, respectively.

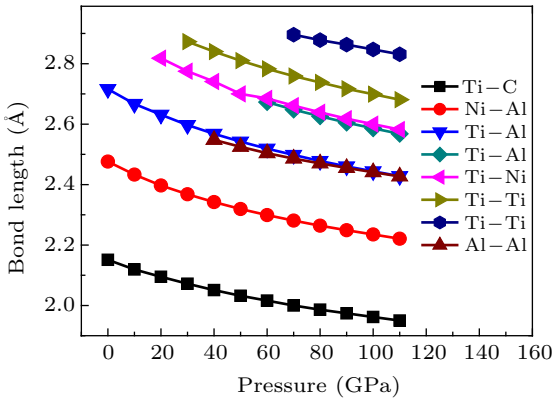


Fig. 2. The bond lengths of quaternary carbide Ti_3NiAl_2C ceramics at different pressures.

The bond lengths of quaternary carbide Ti_3NiAl_2C ceramics decrease with the increasing pressure. At zero pressure, there are three kinds of bonds, namely Ti–Al, Ni–Al, and Ti–C bonds. At pressures of 20 GPa, 30 GPa, 40 GPa, 60 GPa, and 70 GPa, the new bond lengths of Ti–Ni, Ti–Ti, Al–Al, Ti–Al, and Ti–Ti are produced, respectively. At the same time, we can see that the Ti–Ti and Ti–Al bonds appear twice in the process of pressurization. It indicates that pressurization can lead to the diversity of the bonding of quaternary carbide Ti_3NiAl_2C ceramics.

Based on Eqs. (1) and (2), the relationship between volume and pressure can be expressed by the pressure-volume curve. At the same time, we can get these results by fitting the Birch–Murnaghan equation of state. Figure 3 plotted the pressure-volume curve of quaternary carbide Ti_3NiAl_2C ceramics, and the volume decreases with the increasing pressure.

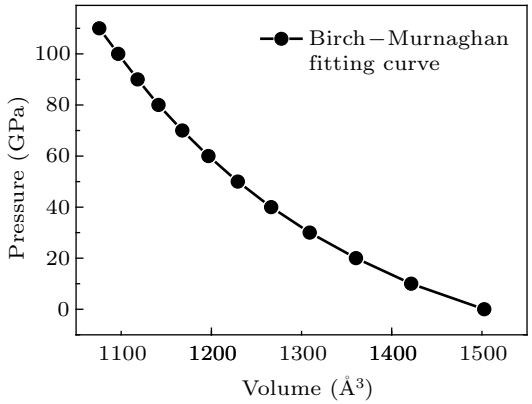


Fig. 3. Birch–Murnaghan fitting curve of quaternary carbide Ti_3NiAl_2C ceramics based on volume (Å^3) and pressure (GPa).

The values of bulk modulus B_0 and its derivative B_0' are listed in Table 1. The value of B_0 at 0 GPa is approximate to the B value in Table 2.

As shown in Fig. 4, we can normalize the lattice constant and volume of quaternary carbide Ti_3NiAl_2C ceramics to investigate the effect of pressure on the cell structure. We can see that the normalization constants of the lattice constant and volume decrease with the increase of pressure. Obviously, the normalization constant of the volume decreases faster. However, we can also see that quaternary carbide Ti_3NiAl_2C ceramics cannot be compressed endlessly. The reason is that as the pressure increases, the volume is continuously compressed, and the bond length between atoms is shortened, which leads to the increase of repulsive force between atoms and makes the crystal difficult to be compressed. We can see from Fig. 4 that the volume of quaternary carbide Ti_3NiAl_2C ceramics is compressed to about 72%.

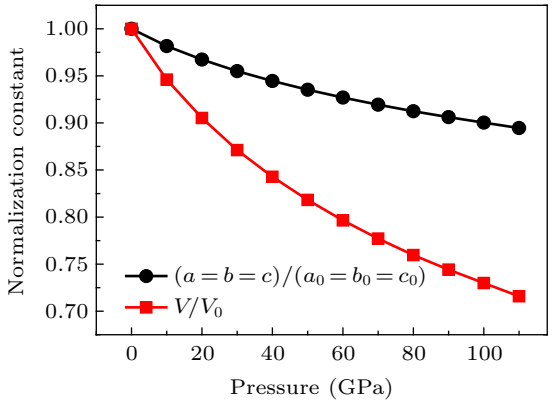


Fig. 4. The normalization parameter of the volumes and lattice constants of cubic Ti_3NiAl_2C compounds at different pressures.

Table 2. Elastic constants (C_{ij}, in GPa), Young's modulus (E, in GPa), shear modulus (G, in GPa), bulk modulus (B, in GPa), B/G ratio, Poisson's ratio (ν), Cauchy pressure (C', in GPa) and anisotropic coefficients (A) of cubic Ti_3NiAl_2C compound at different pressures (GPa).

Pressure	C_{11}	C_{12}	C_{44}	B	G	E	B/G	ν	C'	A
0	278.59	105.7	110.88	163.33	101.11	251.43	1.62	0.243	−2.59	1.28
10	334.70	131.52	134.72	199.24	121.47	302.86	1.64	0.247	−1.60	1.33
20	379.38	159.36	155.94	232.70	137.57	344.76	1.69	0.253	1.71	1.42
30	422.37	186.87	176.11	265.37	152.77	384.52	1.74	0.258	5.38	1.50
40	472.57	208.09	193.95	296.25	169.27	426.57	1.75	0.260	7.07	1.47
50	504.02	237.36	212.36	326.24	180.75	457.72	1.81	0.266	12.50	1.59
60	541.22	261.91	228.85	355.01	193.17	490.55	1.84	0.270	16.53	1.64
70	576.46	286.22	244.56	382.97	204.78	521.41	1.87	0.273	20.83	1.69
80	609.99	310.12	259.39	410.08	215.61	550.37	1.90	0.276	25.37	1.73
90	641.54	333.92	273.38	436.46	225.56	577.23	1.94	0.280	30.27	1.78
100	672.17	357.83	287.00	462.61	235.07	603.06	1.97	0.283	35.41	1.83
110	701.56	381.23	299.89	488.01	244.00	627.43	2.00	0.286	40.67	1.87

3.2. Charge transfer

The charge transfer between atoms can reduce the energy of the compounds to achieve a stable structure. Based on electronegativity analysis, the Ni and C atoms of quaternary carbide Ti_3NiAl_2C ceramics can gain charge, while the Ti and Al atoms can lose charge. Therefore, Ti and Al can produce positive charges, and C and Ni can produce negative charges.

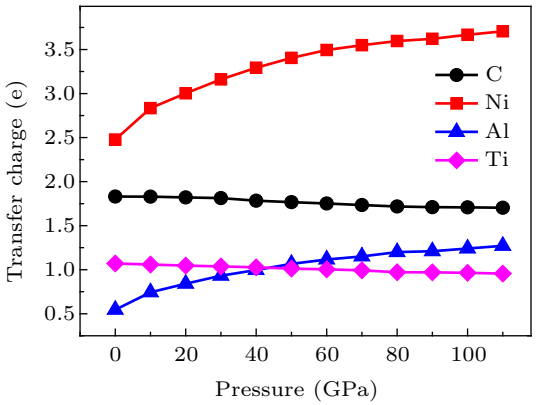


Fig. 5. The transfer charges of quaternary carbide Ti_3NiAl_2C ceramics at different pressures.

As shown in Fig. 5, we investigated the effect of pressure on the charge transfer of quaternary carbide Ti_3NiAl_2C ceramics. According to the Bader charge calculation, we can see that the charge gained by the C atom decreases with the increasing pressure, but the change is not obvious, and the charge transfer is relatively stable. The charge gained by Ni atoms obviously increases with the increasing pressure. Similarly, we can also clearly know that the charge loss of Ti atom decreases with the increase of pressure, but the charge loss is not obvious, and the charge transfer is also relatively stable. However, the charge loss of Al atom obviously increases with the pressure. These results show that pressure has a greater effect on the charge transfer of Ni and Al atoms in cubic Ti_3NiAl_2C compounds, but it has a smaller effect on the charge transfer of C and Ti atoms. How much is the charge transfer? According to Marcus's charge transfer theory, it may be caused by orbital interaction.

3.3. Mechanical properties

Firstly, we fitted the elastic constants of quaternary carbide Ti_3NiAl_2C ceramics at different pressures, and then exported the mechanical parameters such as Poisson's ratio, Cauchy pressure, elastic modulus, and anisotropic factors based on the Eqs. (3)–(10), as shown in Table 2.

The elastic constant C_{11} is often used to characterize the stiffness of compounds. It can be seen from Table 2 that the C_{11} increases with the pressure, indicating that the stiffness of quaternary carbide Ti_3NiAl_2C ceramics can be enhanced by pressurization. C_{12} is generally used to characterize resistance to lateral deformation. Similarly, it can also be seen that the C_{12} increases with the pressure, indicating that pressurization can also increase resistance to lateral deformation. The reason is that pressure makes the bond length shorter, the interaction between atoms is strengthened, and the bond energy also increases, leading to an improvement of the mechanical properties of quaternary carbide Ti_3NiAl_2C ceramics. At the same time, as shown in Table 2, we can also see that the elastic constants of quaternary carbide Ti_3NiAl_2C ceramics at 50–60 GPa are equivalent to that of pure tungsten (Tungsten is considered the most promising first wall material).[56–66]

In addition, the relations $(C_{11}-C_{12})>0$, $C_{11}>0$, $C_{44}>0$, $(C_{11}+2C_{12})>0$ [67] serves as the criterion for determining the mechanical stability of cubic systems. We can deduce that the elastic constants of quaternary carbide Ti_3NiAl_2C ceramics at different pressures obviously meet the stability criteria. It indicates that these structures are mechanically stable. Meanwhile, the phonon dispersion of cubic Ti_3NiAl_2C ceramics (the primitive cell with 28 atoms) at zero pressure is calculated based on density functional perturbation theory (DFPT), as shown in Fig. 6. It is obvious that cubic Ti_3NiAl_2C ceramics is dynamically stable.

Bulk modulus is generally used to evaluate the material's resistance to deformation under external forces.[68,69] We can see from Table 2 that the bulk modulus of quaternary carbide Ti_3NiAl_2C ceramics increases with the increasing pressure, indicating that pressurization can improve the ability to resist deformation. At the same time, it is found that the bulk

modulus (163.3 GPa) at zero pressure is higher than Ti_2AlC (135.8 GPa)[62] and Ti_3AlC_2 (156.2 GPa)[62] ceramics but lower than Ti_3SiC_2 (185.3 GPa)[63] ceramics, which means that cubic Ti_3NiAl_2C ceramics has certain advanced properties. Shear modulus is generally used to characterize the material's resistance to shear deformation.[68,69] We can also see from Table 2 that the shear modulus increases with the pressure, indicating that pressurization can improve the ability of quaternary carbide Ti_3NiAl_2C ceramics to resist shear deformation. Young's modulus corresponds to that of C_{11}, which also characterizes the stiffness of materials. Similarly, we can also see from Table 2 that Young's modulus increases with the pressure, which is equivalent to the conclusion of C_{11}.

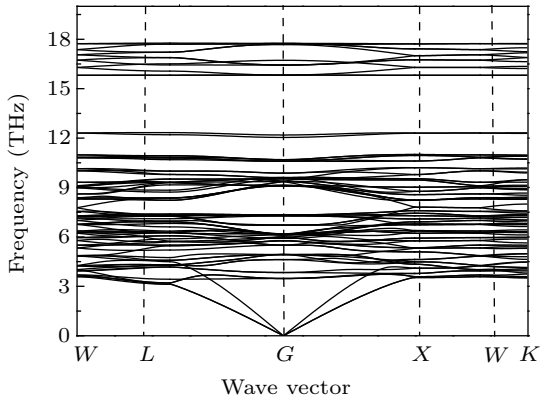


Fig. 6. The phonon dispersion curves of cubic Ti_3NiAl_2C ceramics at zero pressure is calculated based on DFPT.

According to the Pugh theory,[69] the (B/G) ratio can characterize the ductile and brittle behavior of solid materials. 1.75 is usually used to determine whether a material is ductile or brittle. We can see from Table 2 that the B/G value increases with the increase of pressure, indicating that pressurization can improve the ductility of quaternary carbide Ti_3NiAl_2C ceramics. At the same time, we can also see that the B/G values are all lower than 1.75 when the pressure is below 40 GPa, indicating that quaternary carbide Ti_3NiAl_2C ceramics has a brittle phase. However, the brittle phase of the cubic Ti_3NiAl_2C compound changes from brittle to ductile when the pressure reaches 40 GPa. This excellent performance is not available in $M_{n+1}AX_n$ phases, such as Ti_2AlC,[70] Ti_3AlC_2,[70,71] and Ti_3SiC_2[71] compounds at different pressures, which fully reflects the advanced nature of quaternary carbide Ti_3NiAl_2C ceramics. Poisson's ratio is generally used to evaluate the plasticity of solid materials. The quality of plasticity is proportional to Poisson's ratio.[72] Obviously, pressurization can improve the plasticity of quaternary carbide Ti_3NiAl_2C ceramics.

According to the characteristic parameter of Cauchy pressure, it can be determined whether the material has metallic or covalent bond behavior. The positive/negative values of Cauchy pressure indicate that the material has metallic/covalent bond behavior, respectively, as well as ductility/brittleness.[28,73] As shown in Table 2, we can see that Cauchy pressure increases with the pressure, indicating that pressurization can improve the metallic bond behavior of quaternary carbide Ti_3NiAl_2C ceramics. At the same time, we can also see that quaternary carbide Ti_3NiAl_2C ceramics changes from covalent bond to metallic bond at pressure to 20 GPa. Eventually, metallic bonds dominate in the quaternary carbide Ti_3NiAl_2C ceramics.

The material's anisotropy is quantitatively characterized by the anisotropy factor (A). The values of A generally have three types: $A > 1$, $A < 1$, and $A = 1$. $A > 1$ or $A < 1$ indicates that the material has anisotropy, and the greater the deviation from 1, the more severe the anisotropy, and $A = 1$ indicates that the material is isotropic. We can see from Table 2 that the A values increase with the pressure, which indicates that pressurization may aggravate the degree of anisotropy of quaternary carbide Ti_3NiAl_2C ceramics.

3.4. Electronic properties

To further understand the bonding characteristics of quaternary carbide Ti_3NiAl_2C ceramics at different pressures and investigate the mechanical properties and structural stability mechanisms, the total density of states (TDOS) of quaternary carbide Ti_3NiAl_2C ceramics at different pressures (0 GPa, 50 GPa, 80 GPa, 110 GPa) is plotted in Fig. 7. We can see from Fig. 7(a) that the TDOS at the Fermi level has no gap, indicating that quaternary carbide Ti_3NiAl_2C ceramics at different pressures exhibits metallic characteristics. We can also see from Fig. 7(a) that the shape of the TDOS curve changed slightly, which indicates that the structures of quaternary carbide Ti_3NiAl_2C ceramics at different pressures did not change drastically, nor did the structural phase change.

However, as the pressure increases, the TDOS of quaternary carbide Ti_3NiAl_2C ceramics shows a downward trend, which indicates a decreased inter-atomic hybridization energy and weaker inter-atomic hybridization. At the same time, we found that the distance between the valence band and conduction band of the TDOS widens with the pressure, indicating that the delocalization of quaternary carbide Ti_3NiAl_2C ceramics is enhanced.

In general, the TDOS value at the Fermi level (D_f) can indirectly reflect the hardness of the intermetallic, because the hardness is inversely proportional to D_f.[74,75] As shown in Fig. 7(b), The D_f value of quaternary carbide Ti_3NiAl_2C ceramics at the Fermi level decreases with the increasing pressure, which indicates that the hardness increases with the pressure. It is consistent with the trend of elastic constants in Table 2.

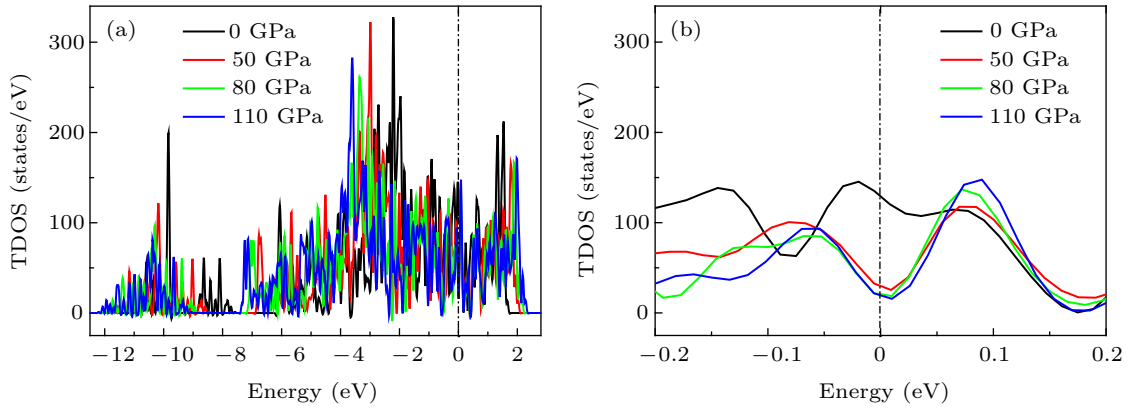


Fig. 7. The total density of states of quaternary carbide Ti_3NiAl_2C ceramics at different pressures (0 GPa, 50 GPa, 80 GPa, 110 GPa). The energy is with respect to the Fermi level.

Table 3. Mass density (ρ, in g·cm^{-3}), Debye temperatures (Θ_D, in K), average wave velocity (v_m), longitudinal sound velocity (v_l), shear sound velocity (v_s), melting point (T_m, in K), and hardness (H, in GPa) of quaternary carbide Ti_3NiAl_2C ceramics at different pressures.

Pressure (GPa)	ρ	Acoustic velocity (m·s^{-1})			Θ_D	T_m	H	H/E	H^3/E^2
		v_s	v_l	v_m					
0	4.75	4612	7920	5117	641	2199	14.0	0.056	0.044
10	5.02	4921	8486	5461	697	2231	15.7	0.052	0.042
20	5.24	5123	8910	5689	737	2495	16.5	0.048	0.038
30	5.45	5296	9280	5885	772	2749	17.3	0.045	0.035
40	5.63	5483	9628	6094	808	3046	18.4	0.043	0.034
50	5.80	5582	9888	6209	832	3232	18.6	0.041	0.031
60	5.96	5694	10139	6336	856	3452	19.1	0.039	0.029
70	6.11	5791	10364	6447	879	3660	19.5	0.037	0.027
80	6.25	5875	10567	6543	898	3858	19.9	0.036	0.026
90	6.38	5948	10752	6626	916	4045	20.1	0.035	0.024
100	6.51	6011	10921	6699	933	4226	20.3	0.034	0.023
110	6.63	6067	11078	6765	947	4399	20.5	0.033	0.022

3.5. Debye temperature, melting point, and hardness

Debye temperature (Θ_D) comes from the atomic thermal vibration theory of solids, which corresponds to the highest frequency of lattice vibration.Θ_D is often used to describe the interatomic bond strength of solid materials.[35,76,77] It is related to many physical quantities of solids, such as hardness, melting point, elasticity, and specific heat. In general, high Debye temperature indicates that solids have high modulus, high melting points and high hardness, and vice versa.

As shown in Table 3, we can see that the Θ_D values increase with the increase of pressure, indicating that pressurization can enhance the Debye temperature of quaternary carbide Ti_3NiAl_2C ceramics. It also indicates that pressurization can increase the strength of the interatomic bonding force.

Melting point (T_m) and hardness (H) are also two critical characteristic parameters of solids. At the same time, H is usually used as an important index to evaluate the wear properties of solids.[78] Herein, it is necessary to investigate the two parameters. Based on the elastic constant C_{11}, shear modulus G, and bulk modulus B, the melting point[79] and Vickers hardness[80] formulas are as follows:

$$T_m = 553\ \text{K} + (5.91\ \text{K/GPa})C_{11} \pm 300\ \text{K}, \quad (15)$$

$$H_V = 0.92\,(G/B)^{1.137}\,G^{0.708}. \quad (16)$$

As shown in Table 3, the melting point and hardness increase with the increase of pressure, indicating that pressurization can enhance the melting point and hardness of quaternary carbide Ti_3NiAl_2C ceramics. In addition, the elastic strain failure (H/E)[19] and the plastic strain failure (H^3/E^2)[19] are usually used to evaluate the wear and resistance to plastic deformation of solids, respectively. It can be seen from Table 3 that the H/E and H^3/E^2 values decrease with the increasing pressure, which indicates that the wear and resistance to plastic deformation of quaternary carbide Ti_3NiAl_2C ceramics may be weakened under pressure.

4. Summary and conclusion

In this paper, we investigate the structural, electronic, mechanical properties, and Debye temperature of quaternary carbide Ti_3NiAl_2C ceramics under high pressure according to the first-principles method. The quaternary carbide Ti_3NiAl_2C ceramics still has a cubic structure under pressure (0–110 GPa). At zero pressure, there are only three kinds of covalent bonds in Ti_3NiAl_2C: Ti–Al, Ni–Al, and Ti–C. However, at the pressures of 20 GPa, 30 GPa, 40 GPa, 60 GPa, and 70 GPa, new Ti–Ni, Ti–Ti, Al–Al, Ti–Al, and Ti–Ti bonds are formed, respectively. The results show that pressurization may result in the bond diversity of quaternary carbide Ti_3NiAl_2C ceramics. When the pressure reaches 20 GPa, the covalent bonds turn into metallic bonds. The volume of quaternary carbide

Ti_3NiAl_2C ceramics can be reduced to 72% of the original volume. The effect of pressure on the charge transfer of Ni and Al atoms in quaternary carbide Ti_3NiAl_2C ceramics is greater than that of C and Ti atoms. The mechanical strength and ductility of quaternary carbide Ti_3NiAl_2C ceramics can be improved by pressure treatment. At 50–60 GPa, its mechanical strength is comparable to that of pure tungsten, and the material changes from brittleness to ductility. However, the anisotropy of quaternary carbide Ti_3NiAl_2C ceramics becomes more serious with the increasing pressure. In addition, pressurization can also improve the Debye temperature, melting point, and hardness of quaternary carbide Ti_3NiAl_2C ceramics, but the wear resistance is decreased.

References

[1] Wang J Y and Zhou Y C 2009 *Annu. Rev. Mater. Res.* **39** 415
[2] Eklund P, Beckers M, Jansson U, Högberg H and Hultman L 2010 *Thin Solid Films.* **518** 1851
[3] Jovic V D, Jovic B M, Gupta S, El-Raghy T and Barsoum M W 2006 *Corros. Sci.* **48** 4274
[4] Was G S, Ampornrat P, Gupta G, Teysseyre S, West E A, Allen T R, Sridharan K, Tan L, Chen Y, Ren X and Pister C 2007 *J. Nucl. Mater.* **371** 176
[5] Barnes L A, Dietz Rago N L and Leibowitz L 2008 *J. Nucl. Mater.* **373** 424
[6] Wang Q M, Garkas W, Renteria A F, Leyens C, Lee H W and Kim K H 2011 *Corros. Sci.* **53** 2948
[7] Haftani M, Saeedi Heydari M, Baharvandi H R and Ehsani N 2016 *Int. J. Refract. Met. Hard Mater.* **61** 51
[8] Barsoum M W, Yoo H I, Polushina I K, Rud V Yu, Rud Yu V and El-Raghy T 2000 *Phys. Rev. B* **62** 10194
[9] Wang X H and Zhou Y C 2010 *J. Mater. Sci. Technol.* **26** 385
[10] Sun Z M 2011 *Int. Mater. Rev.* **56** 143
[11] Xiao J, Yang T, Wang C, Xue J and Wang Y 2015 *J. Am. Ceram. Soc.* **98** 1323
[12] Clark D W, Zinkle S J, Patel M K and Parish C M 2016 *Acta Mater.* **105** 130
[13] Tallman D J, He L, Gan J, Caspi E N, Hoffman E N and Barsoum M W 2017 *J. Nucl. Mater.* **484** 120
[14] Wang C, Yang T, Tracy C L, Xiao J, Liu S, Fang Y, Yan Z, Ge W, Xue J, Zhang J, Wang J, Huang Q, Ewing R C and Wang Y 2018 *Acta Mater.* **144** 432
[15] Su R R, Zhang H L, Shi L Q and Wen H M 2019 *J. Eur. Ceram. Soc.* **39** 1993
[16] Nappé J C, Grosseau Ph, Audubert F, Guilhot B, Beauvy M, Benabdesselam M and Monnet I 2009 *J. Nucl. Mater.* **385** 304
[17] Hoffman E N, Vinson D W, Sindelar R L, Tallman D J, Kohse G and Barsoum M W 2012 *Nucl. Eng. Des.* **244** 17
[18] Tallman D J 2015 *On the Potential of MAX Phases for Nuclear Applications* (Drexel University)
[19] Li W T, Wang Z Y, Shuai J T, Xu B B, Wang A Y and Ke P L 2019 *Ceram. Int.* **45** 13912
[20] Nicolaï J, Furgeaud C, Fonrose B W, Bail C and Beaufort M F 2018 *Mater. Des.* **144** 209
[21] Pazniak A, Bazhin P, Shchetinin I, Kolesnikov E, Prokopets A, Shplis N, Stolin A and Kuznetsov D 2019 *Ceram. Int.* **45** 2020
[22] Pazniak A, Bazhin P, Shplis N, Kolesnikov E, Shchetinin I, Komissarov A, Polcak J, Stolin A, and Kuznetsov D 2019 *Mater. Des.* **183** 108143
[23] Islaka B Y and Ayas E 2019 *Ceram. Int.* **45** 12297
[24] Huang X C, Feng Y, Qian G and Zhou Z J 2019 *Ceram. Int.* **45** 20297
[25] Sridharan S, Nowotny H and Wayne S F 1983 *Monatsh. Chem.* **114** 127
[26] Qin J Q and He D W 2013 *Ceram. Int.* **39** 9361
[27] Feng W X, Cui S X, Hu H Q, Zhang G Q and Lv Z T 2011 *J. Phys. Chem. Solids* **72** 740
[28] Mao P L, Yu B, Liu Z, Wang F and Ju Y 2014 *Comput Mater Sci* **88** 61
[29] Ma Y M, Oganov A R and Xie Y 2008 *Phys. Rev. B* **78** 014102
[30] Xiao H Y, Jiang X D, Duan G, Gao F, Zu X T and Weber W J 2010 *Comput. Mater. Sci.* **48** 768
[31] Ma S Q, Liu Y, Ye J W, Zhang H and Pang J 2014 *Comput. Mater. Sci.* **95** 620
[32] Yuan X L, Wei D Q, Chen X R, Zhang Q M and Gong Z Z 2011 *J. Alloys Compd.* **509** 769
[33] Guo F F, Zhou X L, Li G J, Huang X H, Xue L, Liu D S and Jiang D Y 2020 *Solid State Commun.* **311** 113856
[34] Jiang D Y, Zhong S Y, Xiao W B, Liu D S, Wu M S and Liu S Q 2020 *Int. J. Quantum Chem.* **120** e26231
[35] Qi L, Jin Y C, Zhao Y H, Yang X M, Zhao H and Han P D 2015 *J. Alloys Compd.* **621** 383
[36] Shi S Q, Gao J, Liu Y, Zhao Y, Wu Q, Ju W W, Ouyang C Y and Xiao R J 2016 *Chin. Phys. B* **25** 018212
[37] Feng X K, Shi S Q, Shen J Y, Shang S L, Yao M Y and Liu Z K 2016 *J. Nucl. Mater.* **479** 461
[38] Shang S L, Hector Jr L G, Shi S Q, Qi Y, Wang Y and Liu Z K 2012 *Acta Mater.* **60** 5204
[39] Zhuang Y, Zou Z Y, Lu B, Li Y J, Wang D, Avdeev M and Shi S Q 2020 *Chin. Phys. B* **29** 068202
[40] Shi S Q, Ke X Z, Ouyang C Y, Zhang H, Hangchen Ding H C, Tang Y H, Zhou W W, Li P J, Lei M S and Tang W H 2009 *J. Power Sources* **194** 830
[41] Shi S Q, Zhang H, Ke X Z, Ouyang C Y, Lei M S and Chen L Q 2009 *Phys. Lett. A* **373** 4096
[42] Zhang C Y, Tian F Y and Ni X D 2020 *Chin. Phys. B* **29** 036201
[43] Li W J and Wang C Y 2020 *Chin. Phys. B* **29** 026102
[44] Kresse G and Hafner J 1993 *Phys. Rev. B* **48** 13115
[45] Kresse G and Furthmüller J 1996 *Phys. Rev. B* **54** 11169
[46] Blöchl P E 1994 *Phys. Rev. B* **50** 17953
[47] Wang Y and Perdew J P 1991 *Phys. Rev. B* **44** 13298
[48] Monkhorst H J and Pack J D 1976 *Phys. Rev. B* **13** 5188
[49] Birch F 1978 *J. Geophys. Res.* **83** 1257
[50] Voigt W 1889 *Annalen der Physik (Leipzig).* **38** 573
[51] Reuss A 1929 *Ztschrf. Angew. Math. Mech.* **9** 49
[52] Hill R 1952 *Proc. Phys. Soc. A* **65** 349
[53] Hill R 1963 *J. Mech. Phys. Solids.* **11** 357
[54] Anderson O L 1963 *J. Phys. Chem. Solids* **24** 909
[55] Wachter P, Filzmoser M and Rebizant J 2001 *Physica B* **293** 199
[56] Jiang D Y and Liu S Q 2016 *Rare Metal. Mat. Eng.* **45** 2895
[57] Jiang D Y, Ouyang C Y and Liu S Q 2016 *Fusion Eng. Des.* **106** 34
[58] Jiang D Y, Wang Q L, Hu W, Wei Z Q, Tong J B and Wan H Q 2016 *J. Mater. Res.* **31** 3401
[59] Jiang D Y, Ouyang C Y and Liu S Q 2016 *Fusion Eng. Des.* **112** 123
[60] Jiang D Y, Ouyang C Y and Liu S Q 2017 *Fusion Eng. Des.* **121** 227
[61] Jiang D Y, Zhou Q, Xue L, Wang T and Hu J F 2018 *Fusion Eng. Des.* **130** 56
[62] Jiang D Y, Wang T, Huang X H, Zou X Z and Hu J F 2018 *Fusion Eng. Des.* **137** 295
[63] Jiang D Y, Zhou Q, Liu W H, Wang T and Hu J F 2019 *Physica B* **552** 165
[64] Jiang D Y, Xue L, Huang X M, Wang T and Hu J F 2019 *J. Mater. Res.* **34** 290
[65] Jiang D Y, Wu M S, Liu D S, Li F F, Chai M G and Liu S Q 2019 *Metals* **9** 967
[66] Luo M, Jiang D Y, Liu S Q and Ouyang C Y 2019 *J. Phys. Chem. C* **123** 1913
[67] Wu Z J, Zhao E J, Xiang H P, Hao X F, Liu X J and Meng J 2007 *Phys. Rev. B* **76** 054115
[68] Meradji H, Drablia S and Ghemid S 2004 *Phys. Status Solidi B* **241** 2881
[69] Pugh S F 1954 *Philos. Mag. A.* **45** 823
[70] Gao Q H, Du A and Yang Z J 2017 *Mod. Phys. Lett. B* **31** 1750016
[71] Zhao Y H, Deng S J, Liu H, Zhang J X, Guo Z H and Hou H 2018 *Comput. Mater. Sci.* **154** 365
[72] Cao Y, Zhu J C, Liu Y, Nong Z S and Lai Z H 2013 *Comput. Mater. Sci.* **69** 40
[73] Tang B Y, Yu W Y, Zeng X Q, Ding W J and Gray M F 2008 *Mater. Sci. Eng. A.* **489** 444
[74] Yan M F and Chen H T 2014 *Comput. Mater. Sci.* **88** 81
[75] Wu J Y, Zhang B and Zhan Y Z 2017 *Comput. Mater. Sci.* **131** 146
[76] Tohei T, Kuwabara A, Oba F and Tanaka I 2006 *Phys. Rev. B* **73** 064304
[77] Chen Q, Huang Z W, Zhao Z D and Hu C K 2013 *Comput. Mater. Sci.* **67** 196
[78] Richardson R C D 1967 *Wear* **10** 291
[79] Xu S H, Zhang F Q, Peng P and Liu J S 2010 *Acta Metal. Sinica.* **46** 97
[80] Liu Z T Y, Gall D and Khare S V 2014 *Phys. Rev. B* **90** 134102